International Journal of Thermophysics, Vol. 18, No. 3, 1997

An Equation of State for Two-Center Lennard–Jones Fluids

M. Mecke,[1] A. Müller,[1] J. Winkelmann,[1,2] and J. Fischer[3]

Received August 26, 1996

A new equation of state (EOS) is proposed for the Helmholtz energy F of two-center Lennard–Jones fluids. The EOS is written in the form of a generalized van der Waals equation, $F = F_{\mathrm{II}} + F_{\mathrm{A}}$, where F_{II} accounts for the hard-body interaction and F_{A} for the attractive dispersion forces. The equation is constructed on the basis of previously published data sets and results from new extensive computer simulation studies. It correlates pressures and internal energies over a wide fluid range for two-center model fluids with elongations up to 0.67 in reduced units with a high accuracy and shows an excellent description of the vapor–liquid coexistence properties. Comparisons of results from the new EOS with other data sets and recently published VLE from the NpT plus test particle method show very good agreement.

KEY WORDS: equation of state; Lennard–Jones fluid; molecular simulations; thermodynamic properties.

1. INTRODUCTION

The two-center Lennard–Jones (2CLJ) potential introduced by Sweet and Steele [1] is a widely used model in theoretical and simulation studies on fluids with molecules of nonspherical shape. While in the case of a monatomic Lennard–Jones fluid numerous simulation results are available in the literature which prompted the construction of several equations of state (EOS) [2–6], there was only one EOS published for the 2CLJ fluid by Sowers and Sandler [7]. Their aim was less the construction of a

[1] Institut für Physikalische Chemie, Universität Halle-Wittenberg, Geusaer Strasse, D-06217 Merseburg, Germany.

[2] To whom correspondence should be addressed.

[3] Institut für Land-, Umwelt- und Energietechnik, Universität für Bodenkultur, Peter-Jordan-Strasse 82, A-1190 Wien, Austria.

0195-928X/97/0500-0683$12.50/0

highly accurate EOS than to apply generalized perturbation theory to the development of new equations of state with a very few adjustable parameters. Sowers and Sandler successfully used a three-parameter corresponding-states principle to extend two previously reported equations of state for the monatomic Lennard–Jones fluid [3] to molecular fluids. The three corresponding-states parameters were fitted to simulation data for several model fluids in the supercritical region only. Sowers and Sandler did not include any simulation data for the vapor–liquid equilibrium (VLE) of 2CLJ molecules in their fitting procedure. But just accuracy in the description of the VLE is essential for using the EOS successfully in parameter studies on real fluids or as a basis for extension to dipolar fluids.

Several computer simulation studies were used to describe the vapor–liquid phase equilibrium (VLE) of 2CLJ molecules in the last years. Gupta [8] used thermodynamic integration to calculate Helmholtz free energies. Dubey et al. [9] used the Gibbs ensemble, and recently Kriebel et al. [10] published VLE obtained from the NpT plus test particle method. Moreover, Kriebel [11] generated large data sets for several molecular model fluids covering the whole fluid region. On the other hand, an efficient optimization algorithm developed by Setzmann and Wagner [12] enables us to optimize the form of a complex equation and to determine its parameters. This algorithm was successfully used in the construction of our EOS for a monatomic Lennard–Jones fluid [6].

Hence, we have good basis for the construction of a new equation of state for molecular fluids which shall be able to describe the whole fluid region as well as the vapor–liquid phase equilibria accurately. The new EOS is given in the form of a generalized van der Waals equation, $F = F_H + F_A$, where F_H accounts for the hard-body interaction and F_A for the attractive dispersion forces. We believe this form to be advantageous in study of mixtures if special mixing rules are used for F_H and F_A and, finally, also for the polar contributions to F [13].

2. FUNCTIONAL FORM OF THE EQUATION

We consider a two-center Lennard–Jones (2CLJ) fluid characterized by the parameters ε and σ. The distance between the interaction sites within one molecule is described by the elongation $L = l/\sigma$. We denote all quantities in reduced units, such as the reduced temperature $T^* = kT/\varepsilon$, the reduced density $\rho^* = \rho\sigma^3$, the reduced pressure $p = p\sigma^3/\varepsilon$, and the reduced residual internal energy $u^* = U/N\varepsilon$.

The new equation of state shall be an expression of the residual Helmholtz energy F as a function of the temperature T, the density ρ, and the elongation L,

$F = F(T, \rho, L)$. Furthermore, we want to use the form of a generalized van der Waals equation,

$$F = F_H + F_A \tag{1}$$

where F_H denotes the hard-body contribution and F_A the contribution due to the attractive dispersion forces.

Let us first discuss the hard-body contribution F_H. Accoding to Carnahan and Starling [14] the residual Helmholtz energy of a system of hard spheres with the packing fraction ξ is given by

$$\frac{F_H}{RT} = \frac{(4\xi - 3\xi^2)}{(1-\xi)^2} \tag{2}$$

Boublik and Nezbeda [5] extended this equation to molecular fluids. They considered the core–core distance l by using the anisotropy parameter α and obtained

$$L_H = \frac{l}{d} \tag{3}$$

$$\xi = \frac{\pi}{6}\rho d^3\left(1 + \frac{3}{2}L_H - \frac{1}{2}L_H^3\right) \tag{4}$$

$$\alpha = \frac{(1+L_H)(2+L_H)}{(2+3L_H - L_H^3)} \tag{5}$$

$$\frac{F_H}{RT} = (\alpha^2 - 1)\ln(1-\xi) + \frac{(\alpha^2 + 3\alpha)\,\xi - 3\alpha\xi^2}{(1-\xi)^2} \tag{6}$$

For spherical molecules the anisotropy parameter α becomes 1 and Eq. (6) reduces to the Carnahan–Starling equation, Eq. (2).

Values for the hard-sphere or hard-dumbbell sphere diameter d are obtained from perturbation theories. Owing to the temperature dependence of d, it is useful to have a correlation equation for the packing fraction ξ. Saager et al. [16] developed an equation for ξ based on results of the hybrid Barker–Henderson theory of Smith [17],

$$\frac{(\xi/\xi_0)}{(\rho/\rho_0)} = \left[a + (1-a)\left(\frac{T}{T_0}\right)^\gamma\right]^{-1} \tag{7}$$

with $a = 0.689$, $\gamma = 0.3674$, and $\xi_0 = 0.1617$. For nonpolar substances the quantities T_0 and ρ_0 approximately describe the critical point.

Since exact critical temperatures and densities are very difficult to determine on the basis of computer simulations, we decided to use the so-called pseudocritical quantities obtained by Fischer et al. [8] from perturbation theory studies. While the pseudocritical density ρ_p is nearly equal to the critical density ρ_c, the pseudocritical temperature T_p is known always to be about 15% higher than T_c [18]. Therefore, we have to modify the equation of Saager et al. again. Furthermore, we use correlation functions $f_1(L)$, $f_2(L)$, $f_3(L)$, and $f_4(L)$ given by Eqs. (8)–(11) to describe the quantities ξ_p/ρ_p, T_p, α_p, and ρ_p as functions of the elongation $L = l/\sigma$.

$$f_1(L) = P_1 + P_2 \cdot L^2 + P_3 \cdot L^{2.5} + P_4 \cdot L^4 \tag{8}$$

$$f_2(L) = \begin{cases} (P_5 + P_6 \cdot L)/4(1 + P_7 \cdot L + P_8 \cdot L^2) & \text{for} \quad L = 0.0 \\ (P_5 + P_6 \cdot L)/(1 + P_7 \cdot L + P_8 \cdot L^2) & \text{for} \quad L > 0.0 \end{cases} \tag{9}$$

$$f_3(L) = P_9 + P_{10} \cdot L^2 + P_{11} \cdot L^{3.5} + P_{12} \cdot L^4 \tag{10}$$

$$f_4(L) = (P_{13} + P_{14} \cdot L)/(1 + P_{15} \cdot L + P_{16} \cdot L^2) \tag{11}$$

For the hard-body contribution F_H, we finally obtain

$$\frac{F_H}{RT} = (f_3(L)^2 - 1)\ln(1 - \xi) + \frac{(f_3(L)^2 + 3f_3(L))\,\xi + 3f_3(L)\,\xi^2}{(1 - \xi)^2} \tag{12}$$

$$\xi = \rho^* f_1(L) \left(\frac{1}{0.67793 + 0.32207[T^*/f_2(L)]^{0.3674}} \right) \tag{13}$$

For the description of the attractive dispersion force contribution F_A, we make an ansatz of the form

$$\frac{F_A}{RT} = \sum_i c_i \left(\frac{T^*}{f_2(L)} \right)^{m_i} \left(\frac{\rho^*}{f_4(L)} \right)^{n_i} f_3(L)^{o_i} \exp\left[p_i \left(\frac{\rho^*}{f_4(L)} \right)^{q_i} \right] \tag{14}$$

The powers m_i, n_i, o_i, p_i, and q_i as well as the coefficients c_i are determined by the optimization procedure of Setzmann and Wagner [12].

3. DATA AND OPTIMIZATION PROCEDURE

Although the simple Lennard–Jones fluid has been thoroughly investigated by computer simulations in the last decades, there are very few simulation data available for the 2CLJ fluid. In 1993 Kriebel [11] generated extensive data sets for model fluids of the elongations $L = 0.22$,

Table I. Data Sets Used in the Construction of the Equation of State

L	Source	Number of state points
0.22	Kriebel [11]	51
	This work	98
	Saager and Fischer [22]	46
	Kriebel et al. [10]	16
0.3292	Kriebel [11]	57
	This work	86
0.505	Kriebel [11]	56
	This work	80
	Kriebel et al. [10]	15
0.67	Kriebel [11]	57
	This work	74
	Lustig et al. [23]	19

$L = 0.3292$, $L = 0.505$, and $L = 0.67$. Therefore, these elongations, together with the simple Lennard–Jones fluid treated as a 2CLJ fluid with $L = 0.0$, were chosen to be the bases in the construction of a new equation of state, which consequently should be able to describe two-center molecules of elongations from $L = 0.0$ to $L = 0.67$.

Each data set of Kriebel [11] contains 50 to 60 data points. Although these data cover the entire fluid region, the grid is too wide for the construction of an accurate EOS. So we decided to generate additional data sets for the model fluids $L = 0.22$, $L = 0.3292$, $L = 0.505$, and $L = 0.67$ by NVT molecular dynamics simulations. For each fluid we computed 70 to 100 data points. These data sets as well as the sets of Kriebel [11] together with the concrete simulation conditions are available upon request from the authors on floppy disk. The data sets finally used in the construction of the EOS are shown in Table I. In addition, we used explicitely calculated second virial coefficients as well as VLE data of Kriebel et al. [10]. For the elongation $L = 0.0$ we went back to the data set already used for the construction of our Lennard–Jones EOS, which was recently published [6].

If we reduce T^* and ρ^* to the pseudocritical quantities T_p^* and ρ_p^*, we can specify the ranges of validity of the new equation of state for the 2CLJ fluid in general to

$$0.4 \leqslant T^*/T_p^* \leqslant 5.0$$

$$0.0 \leqslant \rho^*/\rho_p^* \leqslant 3.1$$

For our five model fluids we obtain the ranges given in Table II.

Table II. Ranges of Validity of the New EOS for the Model Fluids Used for Construction

L	T^*	ρ^*
0.00	2.32–29.16	0–0.97
0.22	1.85–23.10	0–0.84
0.3292	1.58–19.71	0–0.75
0.505	1.23–15.39	0–0.63
0.67	1.01–12.68	0–0.54

To get an idea of how the state points are distributed we show in Fig. 1 the grid for one model fluid, $L = 0.3292$. Note that for the 2CLJ model fluids the state point grids are much wider than for the simple Lennard–Jones fluid, for which various data sources are available in literature. Therefore, any data assessment procedure has to be done especially carefully. Incorrect values are often very difficult to recognize due to a lack of state points in direct neighborhood. We have reweighted or excluded only data points which were obviously incorrect and so most of the data remained unchanged.

Let us now have a look at the critical quantities T_c^* and ρ_c^*. For the simple Lennard–Jones fluid several investigations were made to determine these values but the results differ strongly according to the method used by the authors. So we decided to determine the critical point on our own by careful computer simulations in large systems. The method and results are given in an earlier work [6]. However, due to these investigations we

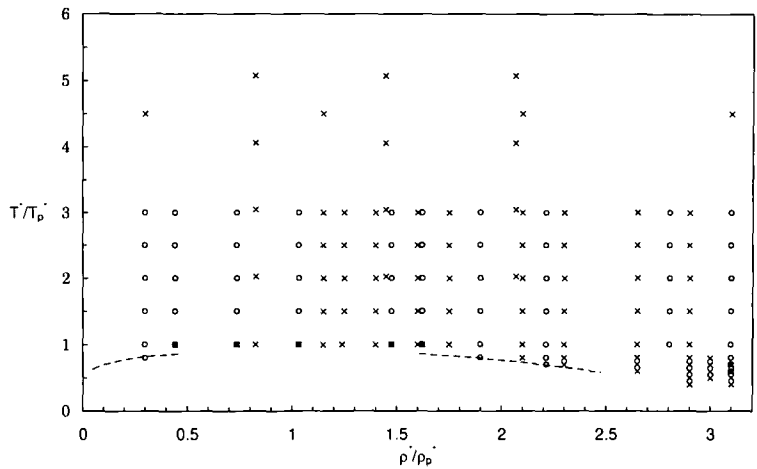

Fig. 1. State point grid for the model fluid $L = 0.3292$ with the simulation points of Kriebel [11] (○) and those of this work (×).

Table III. Coefficients c_i and Powers m_i, n_i, o_i, p_i, and q_i for the Attractive Part of the Helmholtz Energy F_A/RT in Eqs. (14) and (20)

c	m	n	o	p	q
−0.25359778252E+00	−1.5	1	0	0	0
0.94270769752E−02	−1.5	3	−1	0	0
0.10937076431E−03	−1.5	7	−2	0	0
−0.45230360227E−05	−1.5	9	−3	0	0
−0.98945319827E+00	−1.0	1	0	0	0
0.77816220730E+01	−1.0	2	−3	0	0
−0.19338901724E+02	−1.0	2	−2	0	0
0.16188444167E+02	−1.0	2	−1	0	0
−0.47837698146E+01	−1.0	2	0	0	0
−0.37128104806E−05	−1.0	9	−3	0	0
0.11481369341E+01	−0.5	1	−3	0	0
−0.13600256513E+01	−0.5	1	−2	0	0
−0.34629572236E−05	−0.5	9	−3	0	0
−0.48388274860E+00	0.0	1	−3	0	0
0.92061274747E+00	0.0	1	−1	0	0
−0.38763633820E+00	0.0	1	0	0	0
−0.20652959726E+01	0.0	3	1	0	0
0.53102723110E+01	0.0	3	2	0	0
−0.45202666343E+01	0.0	3	3	0	0
0.12858167202E+01	0.0	3	4	0	0
0.31043103969E−03	0.0	5	4	0	0
0.76115392332E−05	0.0	8	−1	0	0
−0.15141679018E+01	−2.0	2	−2	−1	1
0.26132719232E+01	−2.0	2	−1	−1	1
−0.88015285297E+00	−2.0	2	0	−1	1
−0.48730358072E−02	−2.0	5	−1	−1	1
−0.14612399648E−01	0.0	5	3	−1	1
−0.19908427778E−03	0.0	9	2	−1	1
−0.29960728655E+00	−4.0	2	−3	−1	2
0.25016932001E+00	−4.0	2	−2	−1	2
0.16495699794E−01	−4.0	4	−1	−1	2
0.35210453535E+00	−3.0	1	−3	−1	2
−0.43243419699E+00	−3.0	1	−1	−1	2
−0.31194438133E−01	−3.0	4	4	−1	2

estimated the critical point of the Lennard–Jones fluid to be $T_c^* = 1.328$ and $\rho_c^* = 0.3107$. Therefore, we constrained the new EOS for molecular fluids to

$$\left(\frac{\delta P}{\delta \rho}\right)_{T,L}\Bigg|_{T_c^*, \rho_c^*, L_{LJ}} = 0 \tag{15}$$

and

$$\left(\frac{\delta^2 P}{\delta \rho^2}\right)_{T,L}\Bigg|_{T_c^*, \rho_c^*, L_{LJ}} = 0 \tag{16}$$

with $T_c^* = 1.328$, $\rho_c^* = 0.3017$, and $L_{LJ} = 0.0$.

In the case of the other model fluids we find critical quantities given by Gupta [8], Dubey et al. [9], and Kriebel et al. [10], obtained by different simulation methods. As these values also differ strongly, we decided not to use any critical point constraints for one of the other elongations.

To find the contribution of the attractive dispersion forces in the form of Eq. (14), we subtracted the hard-body contributions from the data compiled in Table I from the virial coefficients and from the VLE data of Kriebel et al. [10]. Then we tried to find an optimized ansatz for F_A which simultaneously minimizes the standard deviations of these data. We used the optimization strategy of Setzmann and Wagner [2]. In that procedure, a "bank of terms" is created by prescribed sets for the powers m_i, n_i, o_i, p_i, and q_i in Eq. (14). From this bank of terms the most effective elements are selected by a special search algorithm which combines a stepwise regression analysis with elements of an evolutionary optimization method. Table III contains the powers and coefficients obtained by this procedure for the attractive contribution to the Helmholtz energy F_A given in the form of Eq. (14).

4. DISCUSSION OF THE NEW EQUATION

The new equation of state for molecular fluids is given by Eqs. (17)–(20):

$$F = F_H + F_A \tag{17}$$

$$\frac{F_H}{RT} = (f_3(L)^2 - 1)\ln(1-\xi) + \frac{(f_3(L)^2 + 3f_3(L))\,\xi - 3f_3(L)\,\xi^2}{(1-\xi)^2} \tag{18}$$

$$\xi = \rho^* f_1(L)\left(\frac{1}{0.67793 + 0.32207[T^*/f_2(L)]^{0.3674}}\right) \tag{19}$$

$$\frac{F_A}{RT} = \sum_i c_i \left(\frac{T^*}{f_2(L)}\right)^{m_i}\left(\frac{\rho^*}{f_4(L)}\right)^{n_i} f_3(L)^{o_i} \exp\left[p_i\left(\frac{\rho^*}{f_4(L)}\right)^{q_i}\right] \tag{20}$$

Table IV. Coefficients P_i for the Correlation Eqs. (8)–(11)

i	P_i
1	0.5256
2	3.2088804
3	−3.1499114
4	0.43049357
5	34.0122223
6	17.2324198
7	0.52922987
8	12.7653979
9	1.0
10	0.5296092
11	−0.4531784
12	0.4421075
13	0.3128
14	1.11519758
15	3.48878614
16	6.10644999

Table V. Standard Deviations for the Pressure and the Internal Energy Obtained from the New EOS for the data Sets Used for Construction

Model fluid	$L = 0.0$	$L = 0.22$	$L = 0.3292$	$L = 0.505$	$L = 0.67$
STD_{pT}	1.5746	1.5373	1.9952	1.7733	1.8831
STD_u	1.8645	1.8346	1.9925	1.9360	2.0393

Table VI. Standard Deviations for the Pressure and the Internal Energy Obtained from the New EOS for the Data Set of Müller [19]

L	T^*	ρ^*	p^*_{SIM}	Δp^*_{SIM}	p^*_{EOS}	STD_{pT}	u^*_{SIM}	Δu^*_{SIM}	u^*_{EOS}	STD_u
0.0	4.60	0.822	8.56	0.20	8.622	0.309	−22.114	0.06	−22.0916	0.373
0.1	4.34	0.792	7.92	0.25	8.167	0.988	−21.032	0.06	−20.9868	0.753
0.2	3.80	0.726	6.64	0.20	6.738	0.491	−18.696	0.06	−18.6903	0.096
0.3292	3.11	0.635	5.03	0.15	5.025	0.031	−15.713	0.05	−15.7140	0.021
0.505	2.43	0.533	3.30	0.15	3.336	0.238	−12.771	0.05	−12.7594	0.232
0.67	2.00	0.458	2.02	0.20	2.013	0.037	−10.892	0.05	−10.9000	0.160
0.793	1.77	0.414	1.31	0.20	1.458	0.739	−9.894	0.04	−9.9954	2.534

Table VII. Standard Deviations for the Pressure and the Internal Energy Obtained from the New EOS for the Data Set of Saager and Fischer [20]

T^*	ρ^*	p^*_{SIM}	$\Delta p^*_{\mathrm{SIM}}$	p^*_{EOS}	STD_{pVT}	u^*_{SIM}	$\Delta u^*_{\mathrm{SIM}}$	u^*_{EOS}	STD_u
3.0780	0.06084	0.146	0.002	0.1454	0.291	−1.598	0.045	−1.6122	0.315
4.6170	0.06084	0.263	0.002	0.2617	0.662	−1.351	0.030	−1.3584	0.248
6.1560	0.06084	0.374	0.002	0.3748	0.411	−1.211	0.025	−1.2405	1.181
3.0780	0.14200	0.247	0.007	0.2471	0.009	−3.518	0.045	−3.5474	0.652
4.6170	0.14200	0.594	0.007	0.5917	0.329	−3.096	0.045	−3.0986	0.057
6.1560	0.14200	0.907	0.020	0.9278	1.041	−2.875	0.030	−2.8682	0.227
4.6170	0.20280	0.884	0.020	0.8811	0.146	−4.394	0.045	−4.3857	0.185
6.1560	0.20280	1.491	0.025	1.4593	1.268	−4.085	0.035	−4.0906	0.161
3.0780	0.30420	0.462	0.020	0.4514	0.528	−7.128	0.055	−7.0908	0.677
4.6170	0.30420	1.710	0.015	1.6991	0.730	−6.559	0.030	−6.5523	0.224
6.1560	0.30420	2.918	0.035	2.9067	0.323	−6.106	0.030	−6.1306	0.819
3.0780	0.38532	1.017	0.045	0.9870	0.667	−8.939	0.025	−8.9461	0.286
4.6170	0.38532	3.121	0.070	3.1362	0.216	−8.275	0.015	−8.2816	0.439
6.1560	0.38532	5.188	0.045	5.1572	0.685	−7.669	0.030	−7.6914	0.747
2.1546	0.46644	0.301	0.025	0.2921	0.357	−11.444	0.015	−11.4358	0.546
3.0780	0.46644	2.608	0.035	2.6269	0.540	−10.818	0.015	−10.8122	0.384
4.6170	0.46644	6.168	0.040	6.1466	0.534	−9.872	0.020	−9.8777	0.287
6.1560	0.46644	9.348	0.060	9.3678	0.330	−9.029	0.030	−9.0280	0.032
1.5390	0.54756	0.153	0.050	0.1663	0.265	−14.027	0.025	−14.0093	0.709
2.1546	0.54756	2.907	0.060	2.9775	1.175	−13.352	0.030	−13.3377	0.476
3.0780	0.54756	6.656	0.070	6.7034	0.677	−12.442	0.025	−12.4246	0.694
4.6170	0.54756	12.162	0.080	12.1685	0.081	−11.080	0.030	−11.0775	0.082
6.1560	0.54756	17.085	0.120	17.0720	0.108	−9.857	0.035	−9.8673	0.295
1.5390	0.62868	5.617	0.080	5.5685	0.607	−15.655	0.025	−15.6669	0.477
2.1546	0.62868	9.902	0.090	9.8670	0.389	−14.659	0.030	−14.6742	0.507
3.0780	0.62868	15.446	0.100	15.4906	0.446	−13.370	0.035	−13.3660	0.115
4.6170	0.62868	23.520	0.120	23.6031	0.693	−11.472	0.045	−11.4725	0.010
6.1560	0.62868	30.701	0.140	30.7753	0.530	−9.780	0.045	−9.7964	0.365

and the correlation Eqs. (8)–(11) with the powers and coefficients from Tables III and IV. The ranges of validity are shown in Table II. Here we want to discuss the quality of the new EOS.

First, we investigate how the equation reproduces the data sets used for construction. For that purpose we define standard deviations

$$\mathrm{STD}_{pVT} = \left(\frac{1}{n} \sum_{i=1}^{n} \frac{(p_{i,\mathrm{EOS}} - p_{i,\mathrm{SIM}})^2}{\Delta p^2_{i,\mathrm{SIM}}} \right)^{1/2} \tag{21}$$

and

$$\mathrm{STD}_u = \left(\frac{1}{n} \sum_{i=1}^{n} \frac{(U_{i,\mathrm{EOS}} - U_{i,\mathrm{SIM}})^2}{\Delta U_{i,\mathrm{SIM}}^2} \right)^{1/2} \tag{22}$$

where n denotes the number of state points, and $p_{i,\mathrm{EOS}}$ and $U_{i,\mathrm{EOS}}$ are the results from the EOS, while the simulation results are denoted $p_{i,\mathrm{SIM}}$ and $U_{i,\mathrm{SIM}}$ together with their statistical uncertainties $\Delta p_{i,\mathrm{SIM}}$ and $\Delta U_{i,\mathrm{SIM}}$. The standard deviations for the here considered model fluids are shown in Table V.

Now we are looking for data sets in the literature which were not included in our optimization procedure. Such a data set is given by Müller

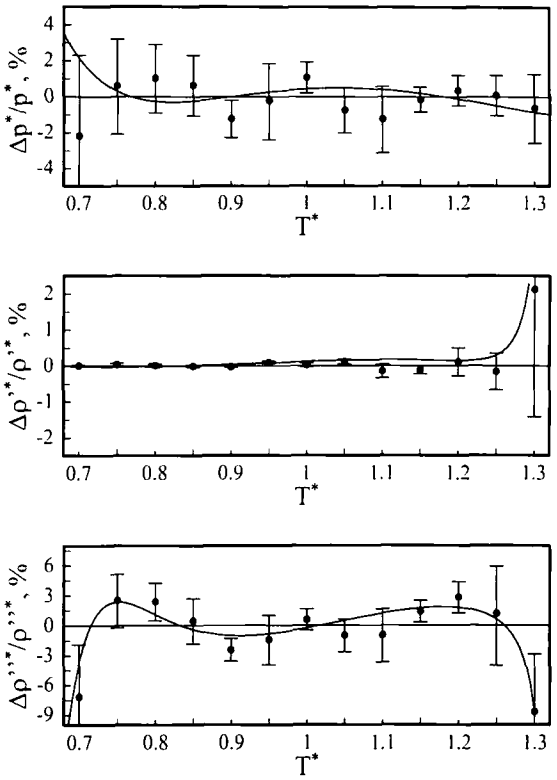

Fig. 2. Deviation plots of the vapor pressures, the saturated liquid densities, and the saturated vapor densities obtained from the new EOS (——) and from direct simulation data [24] (●) in comparison with a correlation equation [24] for the model fluid $L = 0.0$

et al. [19], who performed simulations for a corresponding state point $\rho/\rho_p = 2.628$, $T/T_p = 0.789$. We used these data for computing the standard deviations and show the results in Table VI. We see that all the data up to $L = 0.67$ are reproduced within their simulation uncertainties. Even the values at $L = 0.793$ can be reproduced satisfactorily. There is another data set available from Saager and Fischer [20] for the model fluid $L = 0.505$. Again we can state that the results, given in Table VII, are excellent.

One of the essential points in the discussion of the quality of an equation of state is the description of the vapor–liquid phase equilibrium. Figures 2–6 show the percentage deviations of the vapor pressures, the saturated liquid densities, and the saturated vapor densities obtained from the new EOS and from the correlation equations of Kriebel et al. [10]. We

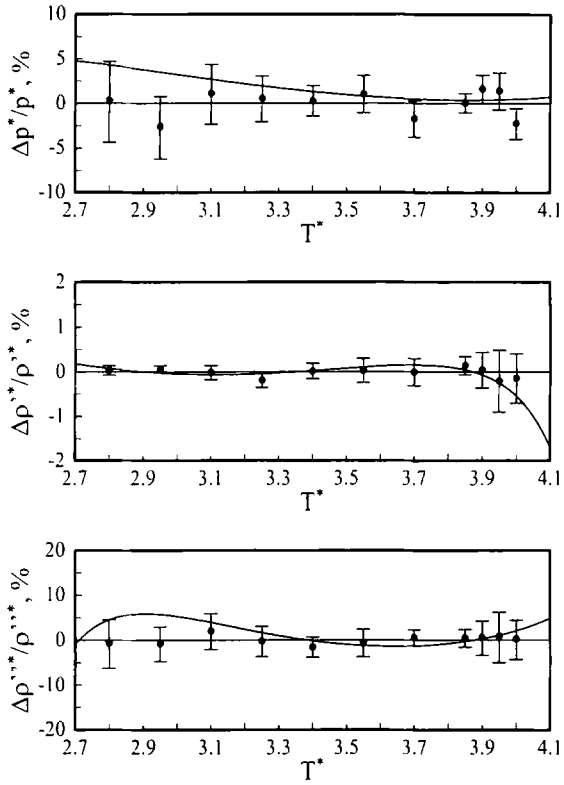

Fig. 3. Deviation plots of the vapor pressures, the saturated liquid densities, and the saturated vapor densities obtained from the new EOS (——) and from direct simulation data [10] (●) in comparison with a correlation equation [10] for the model fluid $L = 0.22$.

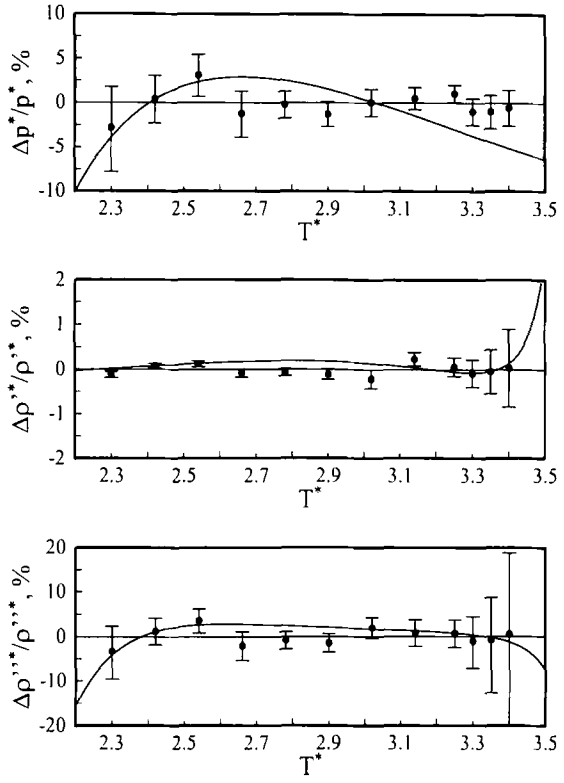

Fig. 4. Deviation plots of the vapor pressures, the saturated liquid densities, and the saturated vapor densities obtained from the new EOS (——) and from direct simulation data [10] (●) in comparison with a correlation equation [10] for the model fluid $L = 0.3292$.

can state that for our model fluids the new EOS is able to describe the phase equilibrium nearly within the simulation uncertainties.

Finally, we show in Table VIII the critical quantities for the model fluids obtained from the new EOS in comparison with the results of Kriebel et al. [10] from the NpT plus test particle method. Kriebel et al. obtained their data from correlations for the saturated vapor density ρ'' and the saturated liquid density ρ' forced into the functional form $\rho' - \rho'' \sim (T_c - T)^{1/3}$. According to experimental evidence, this form holds for nearly infinite ($N \sim 10^{23}$) real systems in the extended critical region. With a decreasing number of particles the critical temperature is believed to increase. Therefore we should expect higher critical temperatures from the equation of state. Except for the elongation $L = 0.22$ we obtain the expected

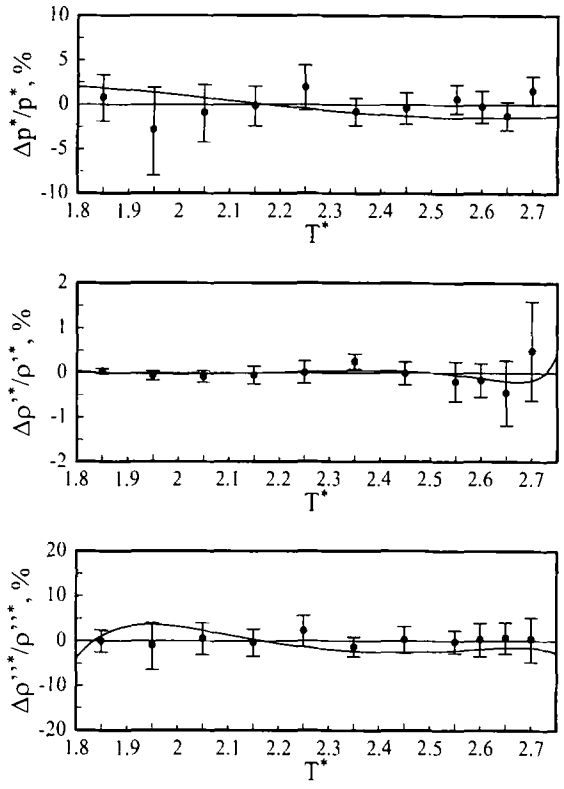

Fig. 5. Deviation plots of the vapor pressures, the saturated liquid densities, and the saturated vapor densities obtained from the new EOS (——) and from direct simulation data [10] (●) in comparison with a correlation equation [10] for the model fluid $L = 0.505$.

behavior. For the model fluid $L = 0.22$ the EOS yields a critical temperature which is somewhat lower than the one from Kriebel et al. [10]. Asking for a reason we should mention the perturbation theory investigations of Bohn et al. [21], who calculated hard-dumbbell diameters and packing fractions at the pseudocritical point as well as pseudocritical densities for several molecular fluids as a function of the elongation L. Bohn et al. find a minimum in the hard-dumbbell diameter at about $L = 0.27$ which causes a maximum in the pseudocritical density. This peculiarity for small elongations could be one reason for the strange behavior we have found. On the other hand, note that we are discussing differences of about 0.7% in the critical temperature. The distance between the critical temperature of Kriebel et al. [10] and their closest simulations is about 7% of T_c^*, and

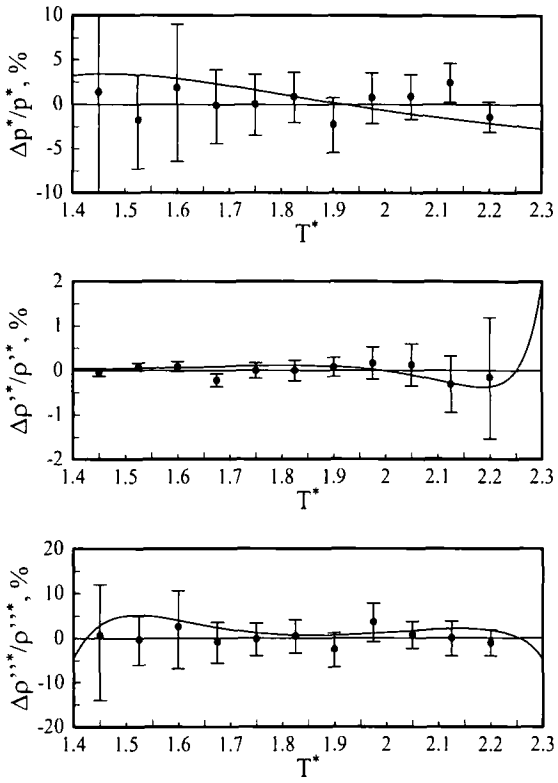

Fig. 6. Deviation plots of the vapor pressures, the saturated liquid densities, and the saturated vapor densities obtained from the new EOS (– – –) and from direct simulation data [10] (●) in comparison with a correlation equation [10] for the model fluid $L = 0.67$.

Table VIII. Critical Points for the Model Fluids Obtained from the New EOS in Comparison with the Results of Kriebel et al. [10]

	Kriebel et al. [10]		New equation of state		
Elongation L	T_c^*	ρ_c^*	T_c^*	ρ_c^*	p_c^*
0.22	4.2931	0.269406	4.264	0.270	0.380
0.3292	3.5436	0.24524	3.602	0.242	0.291
0.505	2.8001	0.20566	2.828	0.203	0.197
0.67	2.3355	0.17526	2.380	0.173	0.147

of course the simulation uncertainties for the coexisting densities increase as one gets closer to the critical point. Therefore, one has to be very careful in trying to explain any peculiarity observed in the critical region.

ACKNOWLEDGMENTS

The authors thank Professor W. Wagner for placing a program package with the optimization algorithm at our disposal. This work was supported by the Deutsche Forschungsgemeinschaft, Az. Wi 1081/1-3 and Fi 287/8-2.

REFERENCES

1. J. R. Sweet and W. A. Steele, *J. Chem. Phys.* **47**:3022 (1967).
2. J. J. Nicolas, K. E. Gubbins, W. B. Streett, and D. J. Tildesley, *Mol. Phys.* **37**:1429 (1979).
3. G. M. Sowers and S. I. Sandler, *Fluid Phase Equil.* **67**:127 (1991).
4. J. K. Johnson, J. A. Zollweg, and K. E. Gubbins, *Mol. Phys.* **78**:591 (1993).
5. J. Kolafa and I. Nezbeda, *Fluid Phase Equil.* **100**:1 (1994).
6. M. Mecke, A. Müller, J. Winkelmann, J. Vrabec, J. Fischer, R. Span, and W. Wagner, *Int. J. Thermophys.* **17**:391 (1996).
7. G. M. Sowers and S. I. Sandler, *Mol. Phys.* **77**:351 (1992).
8. S. Gupta, *J. Phys. Chem.* **92**:7156 (1988).
9. G. S. Dubey, S. F. O'Shea, and P. A. Monson, *Mol. Phys.* **80**:997 (1993).
10. C. Kriebel, A. Müller, J. Winkelmann, and J. Fischer, *Mol. Phys.* **84**:381 (1995).
11. C. Kribel, Dipl.-Chem. thesis (Institut für Physikalische Chemie, Martin Luther-Universität Halle-Wittenberg, Merseburg, 1993).
12. U. Setzmann and W. Wagner, *Int. J. Thermophys.* **10**:1103 (1989).
13. A. Müller, J. Winkelmann, and J. Fischer, *Fluid Phase Equil.* **99**:35 (1994).
14. N. F. Carnahan and K. E. Starling, *J. Chem. Phys.* **51**:635 (1969).
15. T. Boublik and I. Nezbeda, *Coll. Czech. Chem. Commun.* **51**:2301 (1986).
16. B. Saager, R. Hennenberg, and J. Fischer, *Fluid Phase Equil.* **72**:41 (1992).
17. W. R. Smith, in *Specialist Periodical Reports, Statistical Mechanics, Vol. 1*, K. Singer, Ed. (Chem. Soc., London, 1973), p. 71.
18. J. Fischer, R. Lustig, H. Breitenfelder-Manske, and W. Lemming, *Mol. Phys.* **52**:485 (1984).
19. A. Müller, J. Winkelmann, and J. Fischer, *J. Chem. Phys.* **99**:3946 (1993).
20. B. Saager and J. Fischer, *Fluid Phase Equil.* **72**:67 (1992).
21. M. Bohn, B. Saager, K. Holzapfel, and J. Fischer, *Mol. Phys.* **59**:433 (1986).
22. B. Saager and J. Fischer, *Fluid Phase Equil.* **66**:103 (1991).
23. R. Lustig, A. Torro-Labbe, and W. Steele, *Fluid Phase Equil.* **48**:1 (1989).
24. A. Lotfi, J. Vrabec, and J. Fischer, *Mol. Phys.* **76**:1319 (1992).